ChemPubSoc Europe

DOI: 10.1002/chem.201805077

CHEMISTRY
A European Journal
Communication

NMR Spectroscopy

5-Oxyacetic Acid Modification Destabilizes Double Helical Stem Structures and Favors Anionic Watson–Crick like cmo^{5}U-G Base Pairs

Elisabeth Strebitzer[+],[a] Atul Rangadurai[+],[b] Raphael Plangger,[a] Johannes Kremser,[a] Michael Andreas Juen,[a] Martin Tollinger,[a] Hashim M. Al-Hashimi,*[b] and Christoph Kreutz*[a]

Abstract: Watson–Crick like G-U mismatches with tautomeric G^{enol} or U^{enol} bases can evade fidelity checkpoints and thereby contribute to translational errors. The 5-oxyacetic acid uridine (cmo^{5}U) modification is a base modification at the wobble position on tRNAs and is presumed to expand the decoding capability of tRNA at this position by forming Watson–Crick like cmo^{5}U^{enol}-G mismatches. A detailed investigation on the influence of the cmo^{5}U modification on structural and dynamic features of RNA was carried out by using solution NMR spectroscopy and UV melting curve analysis. The introduction of a stable isotope labeled variant of the cmo^{5}U modifier allowed the application of relaxation dispersion NMR to probe the potentially formed Watson–Crick like cmo^{5}U^{enol}-G base pair. Surprisingly, we find that at neutral pH, the modification promotes transient formation of anionic Watson–Crick like cmo^{5}U$^-$-G, and not enolic base pairs. Our results suggest that recoding is mediated by an anionic Watson–Crick like species, as well as bring an interesting aspect of naturally occurring RNA modifications into focus—the fine tuning of nucleobase properties leading to modulation of the RNA structural landscape by adoption of alternative base pairing patterns.

The fidelity of translation relies on the ability of the rigid ribosomal decoding center to recognize the shape of Watson–Crick base pairs.[1] Mismatches can evade these fidelity mechanisms by spatial mimicry of the Watson–Crick like shape through tautomerization and ionization.[2] The propensity to adopt such Watson–Crick like base pairs can be tuned by modifications of the canonical bases at the wobble position to rewire[3] and change the efficiency of translational decoding.[4] Uridine 5-oxyacetic acid (cmo^{5}U) is one such modification that based on X-ray crystallographic and biochemical data has been proposed to increase the efficiency of translation of G-ending codons by promoting formation of Watson–Crick like cmo^{5}U^{enol}-G base pairs.[5] However, because hydrogen atoms could not be visualized by crystallography, the precise nature of the Watson–Crick like species could not be unambiguously determined.

Herein, we have synthesized a ^{15}N isotopically labeled version of the cmo^{5}U modification that allows the application of relaxation dispersion NMR to probe the formation of Watson–Crick like base pairs. Surprisingly, we find that the modification promotes the transient formation of anionic cmo^{5}U$^-$-G base pairs via decreasing the pK_a of the nucleoside. Our results provide key mechanistic insights into how cmo^{5}U influences base-pairing properties and modulates decoding, and lay out a framework for studying the impacts of other RNA modifications.[1]

Our first efforts focused on the synthesis of a $^{15}N_2$-cmo^{5}U phosphoramidite. The synthetic access is loosely based on published syntheses but represents the first comprehensive description of the chemical synthesis of the cmo^{5}U RNA building block. The synthesis started from $^{15}N_2$-uridine, which was prepared according to published procedures by using $^{15}N_2$-urea.[6] In the next steps, the 5-hydroxyl group was installed,[7] followed by protection of the sugar hydroxyls and installation of the 5-oxyacetic acid side-chain as an ester functionality.[8] Removal of the 2′,3′-ketal protecting group was followed by the regioselective incorporation of the 2′-*tert*-butyl-dimethylsilyl group by using a transient 3′,5′-di-*tert*-butylsilyl protection. Then, after removal of the methyl ester functionality, the 4-nitrophenylethylester was obtained via a Steglich esterification. The remaining steps were the introduction of the 5′-(4,4′-dimethoxy)-trityl group and phosphitylation of the 3′-hydroxyl

[a] *E. Strebitzer,[+] R. Plangger, J. Kremser, M. A. Juen, Dr. M. Tollinger, Dr. C. Kreutz*
Institute of Organic Chemistry and
Center for Molecular Biosciences Innsbruck (CMBI)
University of Innsbruck, Innrain 80/82, 6020 Innsbruck (Austria)
E-mail: christoph.kreutz@uibk.ac.at

[b] *A. Rangadurai,[+] Dr. H. M. Al-Hashimi*
Department of Biochemistry and Department of Chemistry
Duke University School of Medicine
Nanaline H. Duke Building, 307 Research Drive, Durham NC 27710 (USA)
E-mail: hashim.al.hashimi@duke.edu

[+] *These authors contributed equally to this work.*

Supporting information and the ORCID identification number(s) for the author(s) of this article can be found under: https://doi.org/10.1002/chem.201805077. It contains experimental details.

group yielding the desired stable isotope modified cmo^{5}U RNA building block. A detailed synthetic scheme and further experimental details on the synthetic steps can be found in the Supporting Information.

Then, the cmo^{5}U modification was introduced into 20 nt RNA model system to probe changes in the overall thermodynamic stability. The cmo^{5}U-modified RNAs were characterized by anion-exchange chromatography and mass spectrometry (Figures S1 and S2 in the Supporting Information). Four RNA constructs differing at the central U5-A16 base pair were synthesized and subjected to UV melting analysis to give the melting temperatures and thermodynamic parameters of the 20 nt hairpins—the U-A hp, the U·G hp, the cmo^{5}U-A hp and the cmo^{5}U·G hp (Figure 1 a–c and Figure S3 in the Supporting

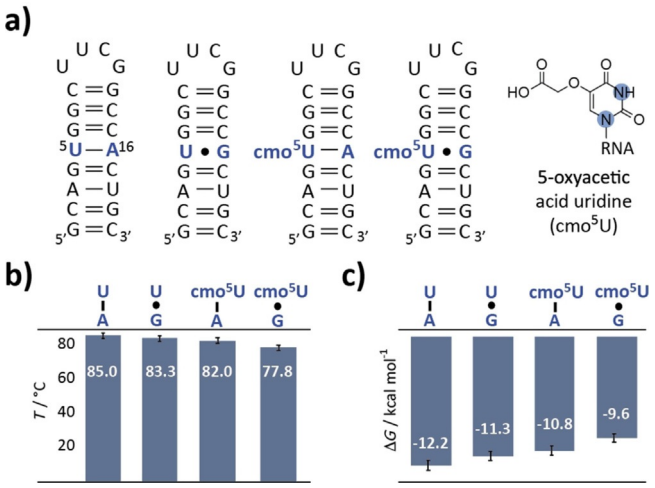

Figure 1. Thermodynamic stability of the unmodified and cmo^{5}U-modified RNAs. a) Secondary structures of the four RNAs under investigation. The inset shows the structure of the cmo^{5}U modification. The nitrogen atoms highlighted in blue are ^{15}N labeled. b) Bar graph of the melting temperatures of the hairpin RNAs. c) Bar graph of the free energies at 298 K of the hairpin RNAs.

Information). As was expected, the U-A hairpin comprising only canonical base pairs showed the highest melting transition at 85 °C and the most negative free energy of −12.2 kcal mol^{-1}, closely followed by the U·G hp (T_m = 83.3 °C, $\Delta G^{298\,K}$ = −11.3 kcal mol^{-1}). The cmo^{5}U-modified hairpins showed slightly decreased stabilities in-line with previously conducted free-energy calculations.[9] The cmo^{5}U-A hp, although forming a canonical base pair exhibits an even lower thermodynamic stability than the U·G hp ($\Delta T_m^{U\text{-}G/cmo5U\text{-}A}$ = 1.3 °C, $\Delta G^{298\,K,U\text{-}G/cmo5U\text{-}A}$ = 0.5 kcal mol^{-1}). The UV melting experiment gives information on the global thermodynamic stabilities of the stem-loop folds, but no structural features and local residue-specific dynamics can be delineated from the UV data.

However, solution NMR spectroscopy is perfectly suited to study structure and dynamics in biomolecules at atomic resolution.[6, 10] Based on NMR data, the U-A hp forms a standard A-form RNA stem capped with an extra-stable UUCG loop. The U·G hp was extensively investigated earlier and in the major populated ground state a U·G wobble base pair was observed.[11] Basically, the same base pairing properties were observed for the cmo^{5}U-modified stem-loop RNAs (Figure 2). The cmo^{5}U-A hp showed slightly shifted imino proton resonances compared to the U-A wildtype sequence, which could be assigned using a ^{1}H-homonuclear NOESY experiment (Figure 2 a,

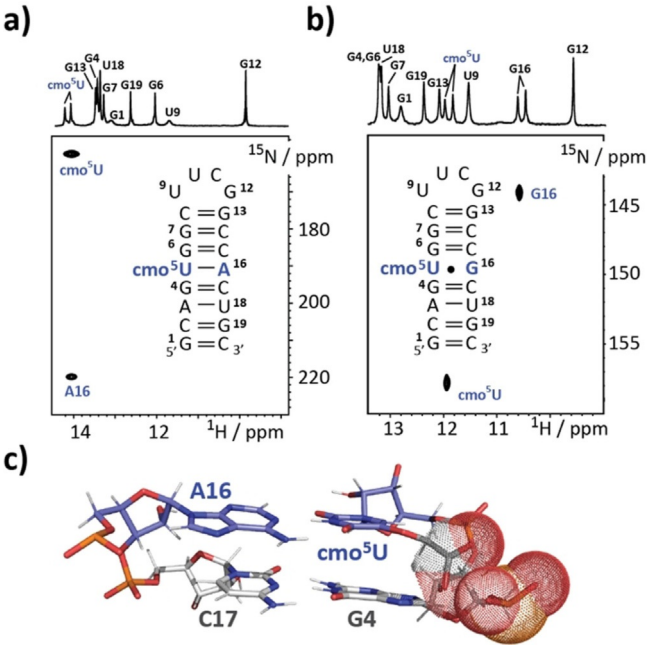

Figure 2. Structural features of cmo^{5}U-modified hairpins. a) Canonical cmo^{5}U-A base pair is observed in an HNN-COSY experiment at 25 °C. b) ^{1}H-^{15}N HSQC data showing chemical shift signatures for the formation of a cmo^{5}U-G wobble base pair (at 5 °C). c) Structural model of the G4-C17 and cmo^{5}U5-A16 base pairs in the cmo^{5}U-A hp. Interfering negative charges of the 5-oxyacetate and the phosphate backbone are shown in dot representation.

upper trace). Noteworthy, the N3H of resonance is shifted from 13.6 ppm (U-A base pair) to 14.1 ppm (cmo^{5}U-A base pair) pointing toward a more de-shielded magnetic environment. We further demonstrated the Watson–Crick like base pairing via an HNN-COSY with residue-specific ^{15}N3 and ^{15}N1 labeling of cmo^{5}U5 and A16, respectively (Figure 2 a). The cmo^{5}U·G wobble base pair was confirmed by ^{1}H-^{15}N-correlation NMR spectroscopy making use of ^{15}N3 and ^{15}N1 labeling of cmo^{5}U5 and G16 (Figure 2 b). Again, a 0.5 ppm de-shielding effect for the cmo^{5}U imino proton resonance (U·G hp U5 H3 11.6 ppm; cmo^{5}U·G hp U5 H3 12.1 ppm) was induced by the 5-oxyacetic acid modification.

We then addressed individual base pair exchange kinetics in all four hairpins by the application of CLEANEX-PM experiments (Table S1 and Figure S4 in the Supporting Information).[12] The slow to very slow imino proton exchange rates between 0.8 to 10 s^{-1} for the U-A hp are in-line with the high thermodynamic stability of the stem loop structure and reveal no dynamic hotspot. In the U·G hp the wobble base pair represents a dynamic base pair opening hot spot with the U5-N3H displaying the highest exchange rate with bulk water protons (22.15 s^{-1}) followed by its interaction partner G16-N3H

(10.14 s^{-1}). The destabilization effect introduced by the U·G wobble appears to be only localized as other imino proton exchange rates are only marginally affected (e.g., U18).

The water-proton-exchange NMR experiment of cmo^{5}U-A hp gave slightly to strongly elevated imino proton water-exchange rates compared to its unmodified U-A counterpart. The cmo^{5}U modification strongly influences the stability of the 5′-preceding base pair—in this case, the G4-C17 base pair. We observed an almost tenfold increase in the water-exchange rate of the G4-N1H proton. A structural model of the cmo^{5}U-A hairpin gives a potential explanation for the destabilization of the 5′-preceding base pair. The model reveals that the negatively charged 5-oxyacetate side chain gets in proximity to the likewise negatively charged phosphate group of G4 (Figure 2c). The repulsion effect induced by this unfavorable electrostatic interaction gives a rational for the tenfold weakening of the G4-C17 base pair and the concomitant global fold destabilization, as has been seen in the UV melting curve analysis. In the thermodynamically most unstable hairpin, the highly dynamic hotspot at the cmo^{5}U·G mismatch site was directly reflected in the imino proton water-exchange rates. We found strongly elevated exchange rates at the mismatch site. Most prominently, the cmo^{5}U5-N3H resonance was strongly broadened at 25 °C preventing the determination of the exchange rate with water protons. The G16 N1H water exchange is sixfold enhanced compared to the U·G wobble base pair (59.88 vs. 10.14 s^{-1}). Again, the destabilization effect introduced by the cmo^{5}U·G wobble is highly localized, because other imino proton water-exchange rates are only marginally affected.

Finally, we addressed the postulated stabilization of the rare enolic uridine state by the cmo^{5}U modification via ^{15}N-$R_{1\rho}$ relaxation dispersion NMR experiments. We previously showed in the hpU·G sequence context (Figure 1a) that the U·G wobble mismatch exists in dynamic equilibrium with two equally populated and rapidly exchanging U-G^{enol} and U^{enol}-G base pairs, with the anionic species falling below detection limits at neutral pH ($p_B < 0.05\%$) and only becoming detectable ($p_B \approx 0.3\%$) at high pH > 7.9.[11]

We examined how replacement of the U·G mismatch with a cmo^{5}U·G base pair affects these dynamics. Strikingly, we found that at neutral pH, the modification significantly increased ^{15}N RD at both cmo^{5}U5-N3 and G16-N1 indicating that it promotes the exchange process to WC-like mismatches (by ca. fivefold, Figure 3a and Table S2 in the Supporting Information). As a negative control, no RD was observed for cmo^{5}U-A hp (Figure S5 in the Supporting Information). Unlike the data for unmodified U·G hp, which could be interpreted in terms of two-state exchange between the wobble and two rapidly exchanging U-G^{enol} and U^{enol}-G base pairs, the RD data for the cmo^{5}U·G hp called for a three-state fit giving two ESs (Table S2 in the Supporting Information). ES1 ($p_B = 0.16 \pm 0.03\%$ and $k_{ex}^{GS\text{-}B} = 5949 \pm 709\ s^{-1}$) has $\Delta\omega$ (cmo^{5}U5-N3) = 16.0 ± 4.8 ppm and $\Delta\omega$ (G16-N1) = 40.4 ± 4.1 ppm consistent with a mixture of rapidly exchanging cmo^{5}U-G^{enol} and cmo^{5}U^{enol}-G and species in a 70:30 ratio. ES2 ($p_c = 0.24 \pm 0.03\%$ and $k_{ex}^{GS\text{-}C} = 976 \pm 683\ s^{-1}$) has $\Delta\omega$ (cmo^{5}U5-N3) = 55.4 ± 2.9 and $\Delta\omega$ (G16-N1) = −0.02 ± 3.5 consistent with the formation of a cmo^{5}U$^-$-G anionic base pair.

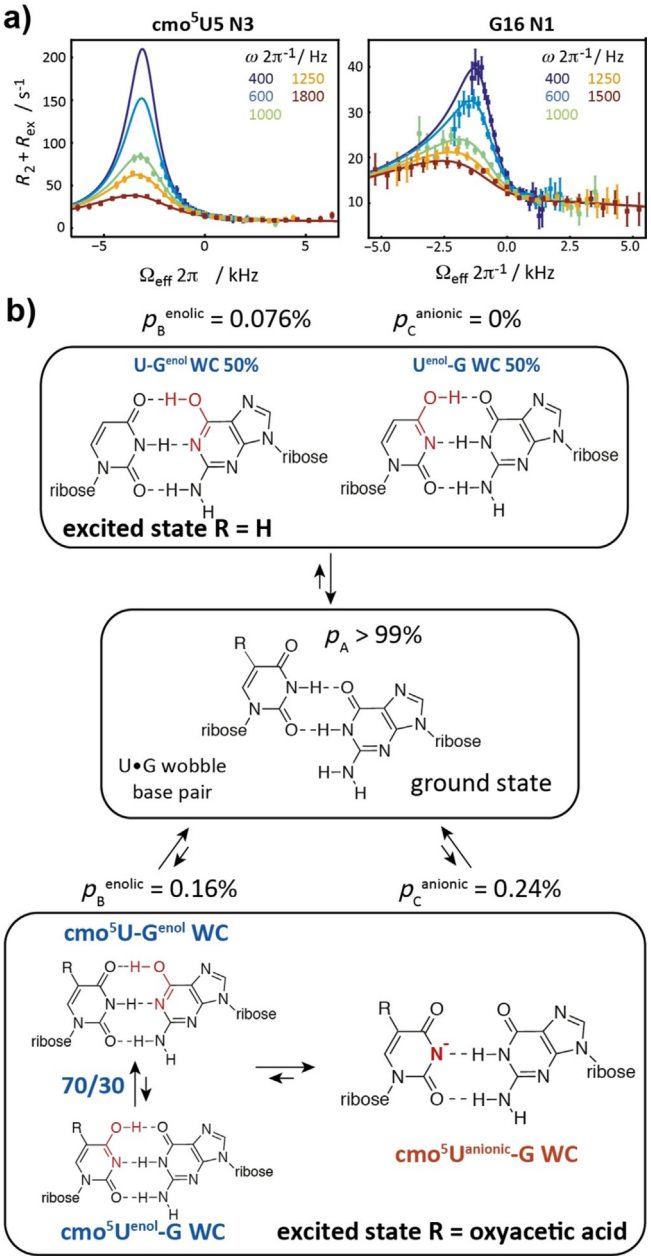

Figure 3. Probing the excited states in cmo^{5}U-modified RNA. a) ^{15}N-$R_{1\rho}$ relaxation dispersion experiments for N3 of cmo^{5}U5 and N1 of G16 with a three-state global fit at pH 6.9 and 10° C. b) Summary on ground/excited state equilibria for the unmodified U-G and the cmo^{5}U-G wobble base pairs.

This was confirmed through measurement of RD profiles at higher pH 8.0 (Table S2 and Figure S6 in the Supporting Information). Therefore, the modification increases the population of the anionic species by > twofold such that it becomes the dominant species in the ES at neutral pH (ca. 60%), although minimally impacting the population of the tautomeric species (ca. twofold) or tautomeric equilibrium (from 50:50 to 70:30 cmo^{5}U-G^{enol}/cmo^{5}U^{enol}-G). These findings are in-line with a recent computational study, in which no evidence for the stabilization of the enolic uridine state by the oxyacetic acid modification was found.[13] They also mirror the effects of 5-bromo-2′-deoxyuridine (5BrdU), which is a mutagenic agent in

DNA that causes increased mis-incorporation via an anionic species.[14] We got further support for the preference of the anionic Watson–Crick like base pairing from the pK_a values determined for the cmo^{5}U nucleoside (Figures S7 and S8 in the Supporting Information). By using pH-dependent ^{13}C NMR data, the pK_a of the 5-oxyacetic acid side-chain was found to be 2.8. Thus, at physiological pH the 5-oxyacetic acid is negatively charged in-line with the observed destabilization effect found for the cmo^{5}U-A RNA. The pK_a of the imino proton H3 in cmo^{5}U is 8.7, that is, the proton is more acidic than in the unmodified uridine nucleoside (pK_a 9.2–9.6) by almost a factor of ten. This higher acidity favors the anionic Watson–Crick like base pair state, as has been seen in the relaxation dispersion data. Further, the higher acidity of the N3-bound proton rationalizes the observed de-shielding effect by the change in its electronic environment.

To conclude, we successfully synthesized a ^{15}N stable isotope labeled variant of a cmo^{5}U RNA building block that allowed to obtain unprecedented insights into the structure and dynamics of RNA carrying this naturally occurring modification via solution NMR spectroscopy. We found a generally destabilizing effect for double helical RNA stem structures by the cmo^{5}U modification very likely due to the additional negative charge introduced by the oxyacetic acid sidechain. The destabilization is reflected in a lowered melting temperature and higher free energy values, and also slightly enhanced imino water proton exchange rates. We further probed the presumed stabilizing effect of the 5-oxyacetic acid modification on the U-enol tautomeric form by ^{15}N-R$_{1\rho}$ relaxation dispersion NMR spectroscopy. We found that an anionic Watson–Crick like cmo^{5}U$^-$-G base pair represents the major species in the excited state. Thus, we have evidence that in a previous work the cmo^{5}U^{enol}-G WC-like base pair was misinterpreted and is in fact an anionic cmo^{5}U-G base pair.[5a] This anionic Watson–Crick base pair between the mRNA and the tRNA anticodon loop might be further stabilized by the controlled conditions regarding pH or metal ion positioning within the ribosome, thus giving an explanation for the expansion of the decoding capacity via the cmo^{5}U modification by a lowered N3H pK_a value.[10] The electron density map in the previous work of Weixlbaumer et al. is also compatible with the anionic base pair formed by N3 and O2 of cmo^{5}U and N1H and N2H of G (Figure 3b).[5a]

Further, the effects of cmo^{5}U in RNA are reminiscent to that of 5-BrdU in DNA, which also promotes formation of an anionic base pair by lowering the pK_a.[14] Thus, cmo^{5}U can be regarded as nature's version of 5-BrdU. Although 5-BrdU is a known chemotherapeutic agent that acts by promoting G point mutations, the function of cmo^{5}U is the enhanced reading capability of G at the third codon position by the formation of an anionic base pair. To summarize, the results highlight an important aspect of the function of naturally occurring RNA modifications—the alteration of the folding landscape of RNA by fine-tuning nucleobases properties leading to alternative base pairing patterns. We are further confident that solution NMR spectroscopy will give important insights into the function of naturally occurring RNA modifications, which is especially important in the light of the recent finding that RNA epigenetics plays an important role in many cellular processes.

Acknowledgments

This work was supported by the Austrian Science Fund (FWF, project P28725 and P30370 to CK) and the Austrian Research Promotion Agency FFG (West Austrian BioNMR, 858017). H.M.A. acknowledges funding from NIH (RO1 GM089846).

Conflict of interest

The authors declare no conflict of interest.

Keywords: NMR spectroscopy · relaxation dispersion · RNA · RNA modifications

[1] A. Rozov, N. Demeshkina, E. Westhof, M. Yusupov, G. Yusupova, *Trends Biochem. Sci.* **2016**, *41*, 798–814.
[2] a) A. Rozov, E. Westhof, M. Yusupov, G. Yusupova, *Nucleic Acids Res.* **2016**, *44*, 6434–6441; b) A. Rozov, P. Wolff, H. Grosjean, M. Yusupov, G. Yusupova, E. Westhof, *Nucleic Acids Res.* **2018**, *46,* 7425–7435.
[3] a) W. A. Cantara, F. V. Murphy, H. Demirci, P. F. Agris, *Proc. Natl. Acad. Sci. USA* **2013**, *110*, 10964; b) T. Muramatsu, K. Nishikawa, F. Nemoto, Y. Kuchino, S. Nishimura, T. Miyazawa, S. Yokoyama, *Nature* **1988**, *336*, 179; c) Y. Ikeuchi, S. Kimura, T. Numata, D. Nakamura, T. Yokogawa, T. Ogata, T. Wada, T. Suzuki, T. Suzuki, *Nat. Chem. Biol.* **2010**, *6*, 277.
[4] a) S. Kurata, A. Weixlbaumer, T. Ohtsuki, T. Shimazaki, T. Wada, Y. Kirino, K. Takai, K. Watanabe, V. Ramakrishnan, T. Suzuki, *J. Biol. Chem.* **2008**, *283*, 18801–18811; b) F. A. P. Vendeix, F. V. Murphy, W. A. Cantara, G. Leszczyńska, E. M. Gustilo, B. Sproat, A. Malkiewicz, P. F. Agris, *J. Mol. Biol.* **2012**, *416*, 467–485; c) D. D. Nedialkova, S. A. Leidel, *Cell* **2015**, *161*, 1606–1618; d) A. Rozov, N. Demeshkina, I. Khusainov, E. Westhof, M. Yusupov, G. Yusupova, *Nat. Commun.* **2016**, *7*, 10457.
[5] a) A. Weixlbaumer, F. V. Murphy IV, A. Dziergowska, A. Malkiewicz, F. A. P. Vendeix, P. F. Agris, V. Ramakrishnan, *Nat. Struct. Mol. Biol.* **2007**, *14*, 498; b) S. J. Näsvall, P. Chen, G. R. Björk, *RNA* **2007**, *13*, 2151–2164; c) S. J. Näsvall, P. Chen, G. R. Björk, *RNA* **2004**, *10*, 1662–1673.
[6] C. H. Wunderlich, R. Spitzer, T. Santner, K. Fauster, M. Tollinger, C. Kreutz, *J. Am. Chem. Soc.* **2012**, *134*, 7558–7569.
[7] T. Ueda, *Chem. Pharm. Bull.* **1960**, *8*, 455–458.
[8] a) J. M. Andrzej, B. Nawrot, E. Sochacka, *Z. Naturforsch. B* **1987**, *42*, 360; b) H. Sierzputowska-Gracz, E. Sochacka, A. Malkiewicz, K. Kuo, C. W. Gehrke, P. F. Agris, *J. Am. Chem. Soc.* **1987**, *109*, 7171–7177.
[9] F. A. P. Vendeix, A. M. Munoz, P. F. Agris, *RNA* **2009**, *15*, 2278–2287.
[10] a) E. S. Szymanski, I. J. Kimsey, H. M. Al-Hashimi, *J. Am. Chem. Soc.* **2017**, *139*, 4326–4329; b) M. A. Juen, C. H. Wunderlich, F. Nußbaumer, M. Tollinger, G. Kontaxis, R. Konrat, D. F. Hansen, C. Kreutz, *Angew. Chem. Int. Ed.* **2016**, *55*, 12008–12012; *Angew. Chem.* **2016**, *128*, 12187–12191.
[11] I. J. Kimsey, K. Petzold, B. Sathyamoorthy, Z. W. Stein, H. M. Al-Hashimi, *Nature* **2015**, *519*, 315.
[12] T.-L. Hwang, P. C. M. van Zijl, S. Mori, *J. Biomol. NMR* **1998**, *11*, 221–226.
[13] Y. D. Hartono, M. Ito, A. Villa, L. Nilsson, *J. Phys. Chem. B* **2018**, *122*, 1152–1160.
[14] I. J. Kimsey, E. S. Szymanski, W. J. Zahurancik, A. Shakya, Y. Xue, C.-C. Chu, B. Sathyamoorthy, Z. Suo, H. M. Al-Hashimi, *Nature* **2018**, *554*, 195.

Manuscript received: October 8, 2018
Accepted manuscript online: October 9, 2018
Version of record online: November 20, 2018

